International Journal of Thermal Sciences 80 (2014) 23–32

Contents lists available at ScienceDirect

International Journal of Thermal Sciences

journal homepage: www.elsevier.com/locate/ijts

Physical quantity synergy analysis and efficiency evaluation criterion of heat transfer enhancement

Lei Ma, Jie Yang, Wei Liu*, Xiaoyu Zhang

School of Energy and Power Engineering, Huazhong University of Science and Technology, Wuhan 430074, China

ARTICLE INFO

Article history:
Received 5 May 2013
Received in revised form
5 October 2013
Accepted 27 January 2014
Available online 4 March 2014

Keywords:
Multi-fields synergy
Efficiency evaluation criterion
Convective heat transfer

ABSTRACT

On the basis of the core-flow heat transfer enhancement and field synergy principle, the difference between fluid-oriented and surface-oriented heat transfer enhancement methods is performed. The physical nature of heat transfer enhancement and friction reduction is illustrated through revealing the synergy principle of heat transfer and friction characteristics of physical quantity and describing the internal relations of velocity and temperature fields as well as velocity and pressure fields. The efficiency evaluation criterion (*EEC*) and the efficiency evaluation plot are proposed to analyze and evaluate heat transfer enhancement techniques corresponding to the different regions in the efficiency evaluation plot. Region I represents the heat transfer enhancement ratio is larger than the pumping power increase ratio and region II represents the heat transfer enhancement ratio is less than the pumping power increase ratio in comparison with a bare tube. 3-D numerical simulations of several inserts in tube are provided to verify multi-fields synergy principle of convective heat transfer and efficiency evaluation plot is carried out to demonstrate the characteristics of enhancement tubes.

1. Introduction

Heat exchangers have been an active subject for applications in engineering field and investigations in academic field in the past several decades. Researches for heat exchangers are aimed at increasing the heat transfer coefficient and decreasing pressure penalty. However, the improved heat transfer techniques prefer to bring heat transfer intensification with the presence of power consumption augmentation in most cases.

There are three aspects on the research for heat transfer enhancement, which are theoretical, numerical and experimental. Theoretically, Bergles [1] divided heat transfer technology into four generations, the first generation of which is bare tube (no fins), the second of which is plain, the third of which is longitudinal vortex generators on fins and the fourth of which is fins with vortex generators subject to electrostatic fields. Specifically speaking, decreasing the thermal boundary layer thickness, extending heat transfer surface area and altering thermal physical property of heat transfer surface are popular ways for heat transfer enhancement [2], which are defined as the boundary layer heat transfer enhancement as the enhanced ways are based on surface [1]. Bejan [3] divided fluid flow into two parts: the boundary flow and the core flow. For the boundary flow heat transfer enhancement, it is common that the ratio of pressure drop increase is always larger than the ratio of heat transfer enhancement. Liu [4–6] analyzed the difference between the boundary flow and the core flow and proposed heat transfer enhancement in the core flow, which is mainly expressed as (1) strengthening temperature uniformity in the core flow; (2) increasing fluid disturbance in the core flow; (3) reducing surface areas of heat transfer elements in the core flow; (4) decreasing fluid disturbance in the boundary flow. Webb [2] proposed three principles of heat transfer enhancement evaluation, which are (1) the size and surface area of the enhanced heat exchangers for the equal pumping power, flow rate and heat transfer rate; (2) the heat transfer rate of the enhanced heat exchangers for the equal size, flow rate and pressure drop; (3) the pressure drop of the enhanced heat exchangers for the equal size, heat transfer rate and fluid rate in comparison with the regular heat exchangers. Guo [7,8] and his co-workers afresh surveyed the physical mechanism of convective heat transfer and proposed a novel concept named field synergy principle for enhancing heat transfer derived from analysis of laminar flow in 2-D flat plate, considering the degree of convective heat transfer is related to the reduction of the intersection angle of velocity and temperature field. According to the field synergy principle, the better the synergy between velocity field and temperature field is, the higher the heat transfer

* Corresponding author. Tel.: +86 27 87542618; fax: +86 27 87540724.
E-mail address: w_liu@hust.edu.cn (W. Liu).

http://dx.doi.org/10.1016/j.ijthermalsci.2014.01.021
1290-0729/

intensification will be under the same boundary conditions of velocity and temperature. As an extension, Tao [9] demonstrated the three mechanisms, i.e. the decreasing the thermal boundary layer, the increasing of the flow interruption and the increasing of the velocity gradient near a heat transfer wall, all lead to the reduction of the intersection angle between the velocity and the temperature field. Numerically and experimentally, lots of research [10–15] such as square ducts, single-phase flow, elliptic tubes, wavy fin heat exchangers with elliptic tubes and fin-and-oval-tube heat exchanger with longitudinal vortex generators is provided according to the theoretical guide. Liu [16–18] developed the principle of synergy and proposed the principle of multi-fields physical quantity synergy for convective heat transfer, introducing more synergy angles on the basis of velocity, temperature and pressure fields and revealing the fundamental nature of heat transfer enhancement and pressure drop reduction. Bejan [19–21] analyzed the entropy generation of heat transfer process based on the second law of thermodynamics and proposed performance evaluation of heat transfer process. It is understood that the detailed methods of heat transfer enhancement can be easily invented once the theoretical research such as enhancement mechanism and evaluation criteria are established. Therefore, the focus of this paper is theoretical analysis with numerical verifications illustrated as follow.

The paper established synergy relation of heat transfer and friction characteristics by analyzing multi-fields for convective heat transfer in tube, based on the core flow heat transfer enhancement and principle of field synergy. The comprehensive value of *EEC* and an evaluation efficiency plot are introduced to evaluate the enhanced techniques. Numerical computations of additives in tube are provided to validate synergy principle and comprehensive efficiency evaluation plot.

2. Physical quantity synergy for convective heat transfer in laminar

The enhancement of convective heat transfer is based on increasing heat transfer coefficient as well as decreasing pressure penalty. For the present enhanced techniques, it is a common knowledge that ratio of flow resistance increment is often larger than the ratio of heat transfer enhancement. Thus it is of considerable significance to enhance heat transfer without much pressure drop augmentation. Based on the internal relations of velocity, temperature and pressure fields, synergy principle of multi-fields for convective heat transfer in laminar flow in tube is introduced.

Refs. [7,8,16–18] proposed the synergy between velocity gradient and temperature gradient and described a dot product of the dimensionless velocity and temperature gradient, which is expressed as:

$$\overline{\boldsymbol{U}}\cdot\nabla\overline{T} = |\overline{\boldsymbol{U}}||\nabla\overline{T}|\cos\beta \tag{1}$$

where $\overline{\boldsymbol{U}}$ and $\nabla\overline{T}$ denote the non-dimensional numbers and definition can be seen in Ref. [17].

For a fixed flow rate and temperature difference in a channel, the smaller intersection angle β between $\overline{\boldsymbol{U}}$ and $\nabla\overline{T}$ is, the larger the dot product $\overline{\boldsymbol{U}}\cdot\nabla\overline{T}$ will be; and the larger Nu is, the more active the convective heat transfer between fluid and a solid wall will be.

Refs. [17,18] proposed the synergy between velocity and pressure gradient, and expressed the synergy relation between velocity vector $\boldsymbol{U}$ and pressure gradient ∇p as:

$$\boldsymbol{U}\cdot(-\nabla p) = |\boldsymbol{U}||-\nabla p|\cos\theta \tag{2}$$

For a fixed flow rate and pressure difference in a channel, the smaller intersection angle θ between $\boldsymbol{U}$ and $-\nabla p$ is, the smaller $|\boldsymbol{U}||-\nabla p|$ will be under fixed $\boldsymbol{U}\cdot(-\nabla p)$. That means less power consumption is employed in the channel.

Based on the analysis of multi-fields synergy for convective heat transfer, two synergy angles of β and θ are introduced to reflect the heat transfer and power consumption characteristics of fluid, revealing the physical nature of heat transfer augmentation and pressure penalty reduction and showing a significance on the design and optimization of heat transfer units and heat exchangers.

3. Heat transfer enhancement in the core flow of a tube

Based on the nature of heat transfer enhancement, Liu [4–6] proposed a principle of heat transfer in the core flow, which is interpolating various heat transfer elements with clearance to the tube wall and enhancing heat transfer in the core flow region, compared with the boundary heat transfer. There are two basic rules for principle of heat transfer enhancement in the core flow, one of which is to improve temperature uniformity and the other of which is to reduce pressure penalty. For the purpose of heat transfer enhancement, the rule of improving temperature uniformity aims at (1) disturbing fluid in the core flow, (2) improving temperature uniformity in the core flow, (3) forming thinner thermal boundary layer near the tube wall, (4) increasing the temperature gradient of thermal boundary layer. Meanwhile, for the purpose of power consumption reduction, the rule of reducing pressure penalty aims at (1) reducing area of additives in the core flow, (2) avoiding disturbance of fluid near tube.

For the boundary flow heat transfer enhancement, due to the elements attached the tube conducting heat flux between fluid to the tube wall, convective heat transfer coefficient between fluid and additives surface can be defined. Whereas, for the core flow heat transfer enhancement, the elements enhancing heat transfer fail to conduct heat flux to tube wall due to the clearance and thus convective heat transfer coefficient between fluid and additives surface does not exist.

In comparison with boundary flow heat transfer, enhancing heat transfer and reducing pressure penalty can be achieved at the same time in the core flow heat transfer, resulting from the fact that a wider region can be taken into account in core flow region to reduce pressure drop and intensify heat transfer by decreasing axial up-coming area and dispersing elements to intensify disturbance to get lower pressure penalty and more vortexes generated in core flow region to get higher convective heat transfer coefficient. Moreover, pressure drop can also be significantly reduced by lower disturbance in boundary layer and less area of elements disturbing fluid.

The above elements of heat transfer enhancement inserted in the core flow of a tube can be divided into two types, one of which is applied to uniform the temperature field, and the other of which is employed to disturb the fluid flow. The elements applied to uniform temperature field, such as porous medium, enhance heat transfer by improving the overall thermal conductivity in the core flow. While the elements employed to disturb the fluid flow, such as twisted tapes and helical screw-tapes, make heat transfer augmentation by disturbing flow and generating vortexes in tube. Synergy angles β and θ vary in the core flow region due to these additives. In this paper, all the following simulations are based on core flow region.

4. Efficiency evaluation criterion and efficiency evaluation plot

He et al. [22] proposed a performance evaluation plot which taking friction factor increase f/f_0 and heat transfer enhancement Nu/Nu_0 as abscissa and ordinate, respectively, and divided the

quadrant of the coordinate into four regions. In region 1 heat transfer is deteriorated without energy-saving based on identical pumping power; in region 2 heat transfer is enhanced based on identical pumping power; in region 3 heat transfer is enhanced based on identical pressure drop; in region 4 heat transfer enhancement ratio is larger than friction factor increase ratio based on identical flow rate.

Webb [23,24] gave the precise definition of comprehensive evaluation index *PEC* in common use as follows:

$$PEC = \frac{hA/h_0A_0}{(P/P_0)^{1/3}(A/A_0)^{2/3}} = \frac{Nu/Nu_0}{(f/f_0)^{1/3}(Re/Re_0)(Pr/Pr_0)^{1/3}} \quad (3)$$

where *Nu*, *Re* and *Pr* denote the Nusselt number, Reynolds number and Prandtl number of flow, respectively; *P* is the power consumption of fluid; *h* is the coefficient of convective heat transfer; *A* is the heat transfer area and *f* is the friction factor defined as follow,

$$f = 2D\Delta p/\left(\rho u_m^2 L\right) \quad (4)$$

where *D* denotes the hydraulic diameter, Δp is the difference value of pressure from inlet to outlet. u_m represents the average velocity of cross-section. *L* is the length of a tube.

All physical quantities related to a bare tube will be denoted by a subscript 0. For the same *Re* number, when the property of fluid remains unchanged and the heat transfer area is fixed, the power consumption will be fixed. According these assumptions, Equation (3) can be rewritten as:

$$PEC = \frac{Nu/Nu_0}{(f/f_0)^{1/3}} \quad (5)$$

Here, we use efficiency evaluation criterion as:

$$EEC = \frac{Q/Q_0}{(V\Delta p)/(V_0\Delta p_0)} \quad (6)$$

where *Q* is heat flux and *V* is volume flow rate. The numerator Q/Q_0 represents the ratio of heat flux of enhanced tube over a bare one and the denominator $(V\Delta p)/(V_0\Delta p_0)$ represents the ratio of corresponding pump power consumption of an enhanced tube over a bare one. *EEC* can also clearly represent the comprehensive performance of a heat transfer unit.

The Reynolds numbers of a bare tube and an enhancement tube are always set as identical in the experiment of heat transfer and friction characteristics. The volume flow rate is identical based on identical pipe diameter with the same Reynolds number, so *EEC* can be rewritten as:

$$EEC = \frac{Q/Q_0}{\Delta p/\Delta p_0} \quad (7)$$

Eq. (7) represents the quotient of profit ratio between the enhanced and bare tubes by heat transfer enhancement and cost ratio by power consumption. Apparently, *EEC* is derived from the angle of the ratio of profit and cost.

By taking the decadal logarithm of Eq. (7), we have:

$$\lg\left(\frac{Q}{Q_0}\right) = \lg\left(\frac{\Delta p}{\Delta p_0}\right) + \lg(EEC) \quad (8)$$

If we take $\lg(\Delta p/\Delta p_0)$, $\lg(Q/Q_0)$ as the abscissa and ordinate respectively, then Eq. (8) represents a straight line for which slope is 1 and the intercept of it is the value of *EEC* in such a coordinates system. When $EEC = 1$, i.e. $\lg(EEC) = 0$, the straight line crosses origin (1, 1), that means that the profit ratio by heat transfer enhancement is equal to the cost ratio by power consumption. Meanwhile, the straight line divides the plot into two regions as shown in Fig. 1 and is called baseline for clarity. Obviously, in region I the heat flux ratio is larger than power consumption ratio while in region II the heat flux ratio is less than power consumption ratio between the enhanced and bare tubes.

According to the previous introduction, the comprehensive efficiency evaluation plot is proposed in Fig. 1 which takes $\lg(\Delta p/\Delta p_0)$ and $\lg(Q/Q_0)$ on identical Reynolds number as the abscissa and ordinate. Broadly speaking, the ratio of power consumption increase is often larger than the ratio of heat transfer enhancement, thus most of working points of enhancement techniques are located in region II, practically. Therefore, a certain heat transfer enhancement technique of which the working points are located in region I or approach region I, i.e. *EEC* is larger than 1 or close to 1, is preferable and applicable for energy-saving purpose since the ratio of heat transfer enhancement is larger than the ratio of power consumption increase.

According to the above discussion, the ratio of heat transfer augmentation and the ratio of power consumption increase based on identical Reynolds number can be obtained in Fig. 1 for a certain working point **A**. Moreover, the intercept of the line with point **A** located which is parallel with baseline is the value of *EEC*. Therefore, ratio of heat flux increase, ratio of pumping power augmentation and the value of comprehensive *EEC* based on identical Reynolds number can be obtained by the location of a working point on the efficiency evaluation plot and thus enhanced heat transfer techniques are evaluated effectively.

Some examples of numerical simulations are illustrated as follows based on the analysis of multi-fields physical quantity synergy and of efficiency evaluation criterion in the core flow convective heat transfer.

5. Numerical simulation of convective heat transfer enhancement in tube

The commercial software Fluent 6.3.26 is chosen as the computation tool in this work to analyze the heat transfer enhancement techniques aimed at energy-saving, size and cost reduction and efficiency improvement. Based on the core flow heat transfer enhancement, the paper provides various additives in the core flow to verify multi-fields physical quantity synergy principle and efficiency evaluation plot. In the paper, elements intensifying fluid disturbance and elements improving temperature uniformity are presented in Refs. [25–28], respectively. Entrance region of tube

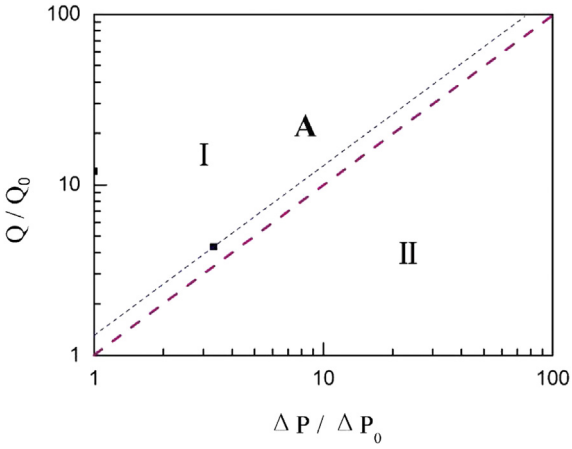

Fig. 1. Comprehensive efficiency evaluation plot.

is used for simulation rather than fully developed region in this paper. To simplify numerical simulations, the following assumptions are made: (1) the thermal–physical properties of fluid such as ρ, μ, c_p, k are constant; (2) fluid is incompressible, isotropic and continuous; (3) fluid is Newtonian fluid; (4) the effect of gravity is negligible; (5) the flow state is steady; (6) take tube inlet Reynolds number as the overall Reynolds number, neglecting the influence caused by additives for fluid; (7) heat conduction in additives is neglected.

Equations of the continuity, momentum and energy for the fluid flow are given below in a tensor form.

Continuity equation:

$$\frac{\partial(\rho u_i)}{\partial x_i} = 0 \tag{9}$$

Momentum equation:

$$\frac{\partial}{\partial x_j}(\rho u_i u_j) = -\frac{\partial p}{\partial x_i} + \frac{\partial}{\partial x_j}\left[\mu\left(\frac{\partial u_i}{\partial x_j} + \frac{\partial u_j}{\partial x_i}\right)\right] \tag{10}$$

Energy equation:

$$\frac{\partial}{\partial x_j}\left(\rho u_j c_P T - k\frac{\partial T}{\partial x_j}\right) = 0 \tag{11}$$

All the boundary conditions for numerical simulations of different tube additives are set as the same way as follows: the finite difference method and the two-order upwind difference scheme are applied to the numerical computation, and the SIMPLE algorithm is used for the coupling between pressure and velocity fields; the two-order upwind difference scheme is applied for energy and momentum, and the standard difference scheme is used for the pressure field; tube wall temperature $T_w = 350$ K, and inlet temperature of fluid $T_\infty = 293$ K; the surface of tube additives is set to be adiabatic in stable flow; the working fluid is water and inlet Reynolds numbers are set as 300–1800 in laminar flow. In addition, convergence criteria of 10^{-6} for the continuity and velocity components and 10^{-8} for energy are applied, respectively. All the following models are used in the same grid system with non-uniform structured mesh generated by Gambit 2.0. Compared with the theoretical data, the grid independent work has been done in Ref. [28]. The correlation data and experimental results have been compared to the computational models in Refs. [28,29] to verify the precision on predicting heat transfer and hydraulic performance. The identical modeling approach was adopted in the present work.

5.1. Three regularly-spaced twisted tapes in a tube

Three regularly-spaced twisted tapes are presented in a tube as shown in Fig. 2. The twisted tapes have the geometric dimensions of $L = 500$ mm, $D = 20$ mm, $t = 1$ mm, $W = 4$ mm, $L_h = 20$ mm, $L_s = 5$ mm and are placed at the corners of an equilateral triangle. The distance a between each twisted tapes in the cross section is 5 mm, 6 mm and 7 mm, respectively.

Heat transfer and friction characteristics for three twisted tapes in a tube are presented in Fig. 3(a) and (b). As shown in the figure, Nusselt number increases slightly as the distance between twisted tapes in the cross section varies from 5 mm to 7 mm. Apparently, since heat transfer enhancement is intensified with the increase of Reynolds number, Nusselt number increases significantly with the increase of Reynolds number and reaches the maximum value at about 90 when $Re = 1800$. Meanwhile, the friction factor increases as the space between twisted tapes in the cross section varies from 5 mm to 7 mm and decreases significantly with the increase of Re. The friction factor reaches the minimum value at about 0.3 when $Re = 1800$ and $a = 5$ mm.

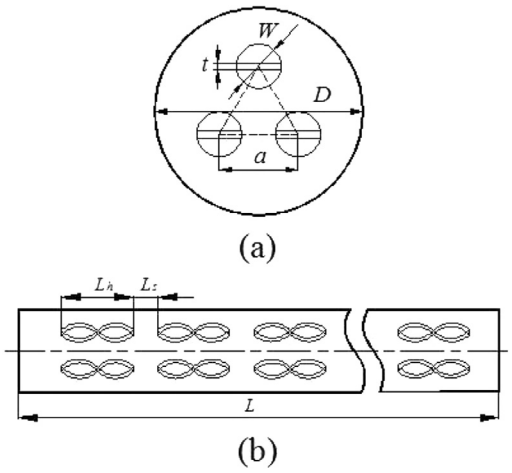

Fig. 2. Three regularly-spaced twisted tapes in tube, (a) cross section geometric dimension; (b) axial geometric dimension.

Fig. 3(c) and (d) show the synergy angle β and θ as a function of Reynolds number for three twisted tapes in a tube. For a bare tube, the synergy angle β and θ keep about 88.8°–88.9° and 0.93°–1.2°, respectively, under different Re numbers. As shown in the figure, synergy angle β, which reaches the maximum value when $a = 5$ mm and minimum value when $a = 7$ mm on identical Reynolds number, decreases with increase of Re and the average value is about 81°. Apparently, the decrease of synergy angle β corresponds to the increase of Nusselt number at various Reynolds numbers. While synergy angle θ increases with increase of Reynolds number and reaches the maximum value when $a = 7$ mm and minimum value when $a = 5$ mm on identical Reynolds number. Apparently, the increase of synergy angle θ corresponds to the increase of friction factor at various Reynolds numbers.

Fig. 4 shows the relation of EEC value with Reynolds number for three twisted tapes in a tube. As show in the figure, the enhanced tube with three twisted tapes shows a high value of EEC and it increases with the increase of Reynolds number. It turns out the maximum value is 1.194 when $Re = 1800$ and $a = 5$ mm, i.e. compared with a bare tube, the ratio of heat flux augment is 1.194 times as the ratio of power consumption increase. According to the above analysis, three twisted tapes in a tube present an expecting result for the purpose of energy-saving and are applicable in engineering fields.

5.2. Four regularly-spaced twisted tapes in a tube

Four regularly-spaced twisted tapes are arranged in a tube as shown in Fig. 5. Compared to the three twist tapes, the four twisted tapes has the geometric dimensions of $L = 500$ mm, $D = 20$ mm, $t = 1$ mm, $W = 4$ mm, $L_h = 20$ mm, $L_s = 5$ mm. The distance between each twisted tapes in the cross section is also 5 mm, 6 mm and 7 mm, respectively.

Heat transfer characteristics and synergy for four twisted tapes in a tube are presented in Fig. 6(a) and (b). The trend of computational results is similar to that of three twisted tapes in a tube. Nusselt number, which increases with the increase of Reynolds number, increases slightly as the distance between twisted tapes in the cross section varies from 5 mm to 7 mm and reaches the maximum value about 105 when $Re = 1800$. At the same time,

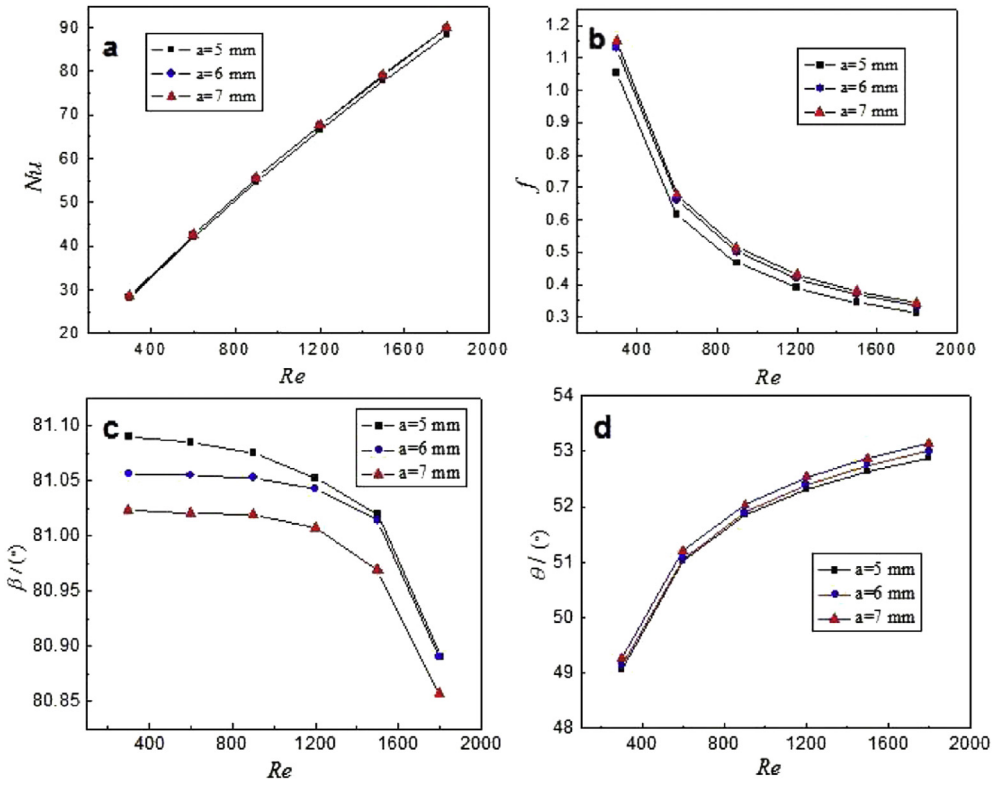

Fig. 3. Relation between *Re* and *Nu*, *f*, β, θ of heat transfer enhanced tube with three twisted tapes in (a), (b), (c), (d) respectively.

β decreases slightly with the increase of *Re* and reaches the minimum value when $a = 7$ mm and maximum value when $a = 5$ mm. Apparently, the decrease of synergy angle β corresponds to the increase of Nusselt number as a function of various Reynolds numbers.

Friction characteristics and synergy for four twisted tapes in a tube are presented in Fig. 6(c) and (d). The friction coefficient decreases with Reynolds number ranging from 300 to 1800 and reaches maximum and minimum when $a = 7$ mm and $a = 5$ mm, respectively.

Fig. 7 shows the relation of *EEC* value with Reynolds number for four twisted tapes in a tube. As shown in the figure, the comprehensive efficiency index of four twisted tapes in a tube increases with increase of *Re* and gives the maximum *EEC* value 1.05 when $Re = 1800$ and $a = 5$ mm, i.e. in comparison with a bare tube, the ratio of heat transfer enhancement is 1.05 times as the ratio of power consumption increase. The *EEC* value is slightly less than that of three twisted tapes in a tube but it is still applicable and practical in engineering fields for the purpose of energy-saving.

5.3. Triangle poles and ten crossing poles insert in a tube

Regularly-spaced triangle circular poles and ten crossing circular poles are placed in tubes as shown in Figs. 8 and 9. The model has the geometric dimensions of $D = 20$ mm, $L = 500$ mm,

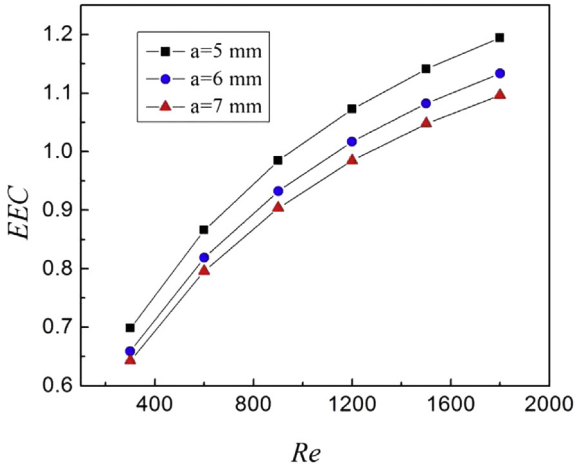

Fig. 4. Relation between *Re* and *EEC* of heat transfer enhanced tube with three twisted tapes.

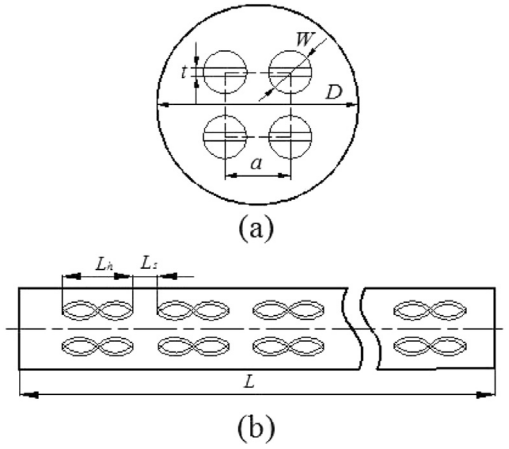

Fig. 5. Four regularly-spaced twisted tapes in tube, (a) cross section geometric dimension; (b) axial geometric dimension.

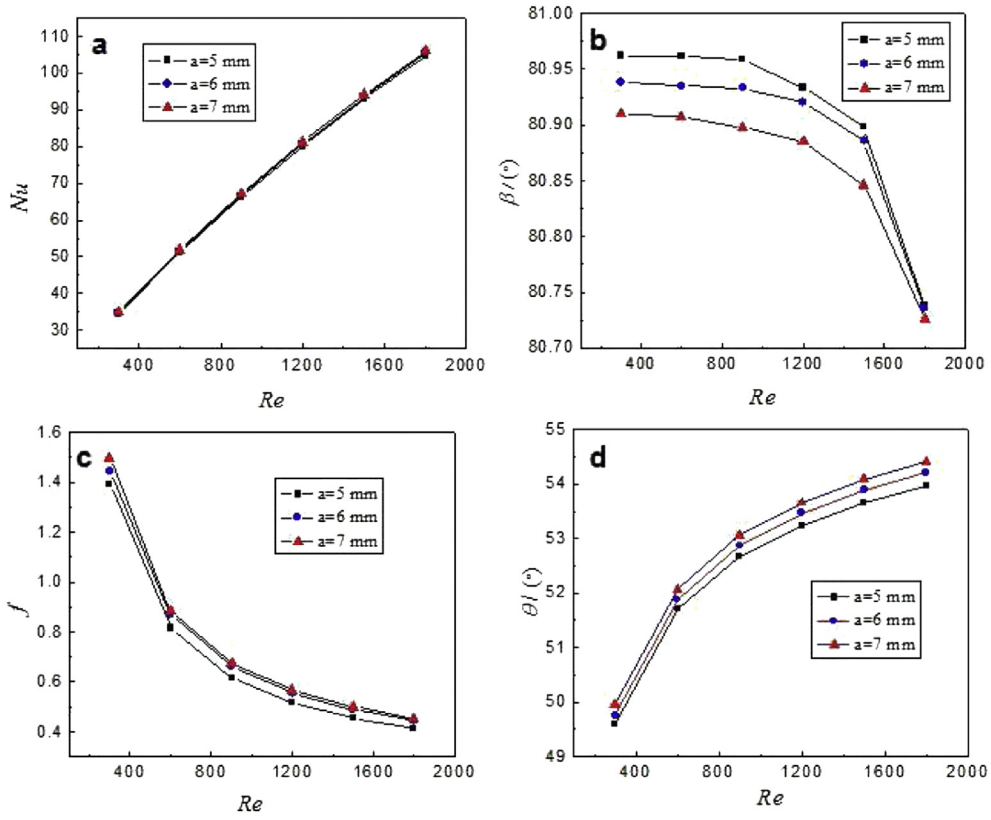

Fig. 6. Relation between *Re* and *Nu*, β, *f*, θ of heat transfer enhanced tube with four twisted tapes in (a), (b), (c), (d) respectively.

$s = 12.5$ mm, $d = 1$ mm. The distance from the end of pole to the tube wall is 1 mm. The inserting additives are arranged in staggered pattern.

As shown in Fig. 10, heat transfer performance of triangle circular poles is better than that of ten crossing circular poles, corresponding to synergy angle β. For triangle circular poles inserting a tube, Nusselt number reaches about 62 and synergy angle β reaches about 83.5° when $Re = 1800$. The friction factor of triangle circular poles is larger than that of ten crossing circular poles, corresponding to θ. For ten crossing circular poles inserting a tube, the friction factor reaches about 0.45 and synergy angle θ reaches about 48.5° when $Re = 1800$.

Fig. 11 shows the relation of *EEC* value with Reynolds number for triangle circular poles and ten crossing circular poles inserting in a tube. As shown in the figure, the *EEC* value of triangle circular poles in a tube increases with Reynolds number, which ranges from 300 to 1200, and remains constant near about 0.49 once Reynolds number exceeds 1200. The *EEC* value of cross circular poles in a tube increases with Reynolds number, which ranges from 300 to 1800, and reaches the maximum value 0.572. Accordingly, the model of triangle circular poles and ten crossing circular poles inserting in a tube for the purpose of energy-saving is not applicable due to the low *EEC* value.

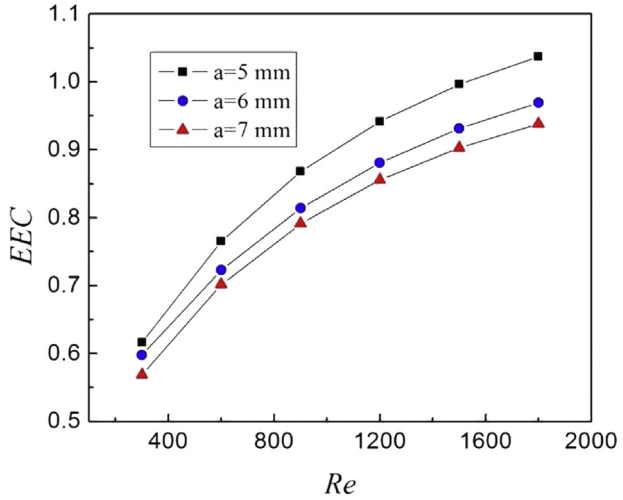

Fig. 7. Relation between *Re* and *EEC* value of heat transfer enhanced tube with four twisted tapes.

5.4. Screw-tape in tube

Full-length helical screw-tapes and regularly-spaced helical screw-tapes are arranged in a tube as shown in Fig. 12. The model has the geometric dimensions of $D = 20$ mm, $L = 500$ mm, $W = 10$ mm. The thickness of helical screw-tapes d is 1 mm. Regularly-spaced helical tapes has the geometric dimensions of L_h=54 mm and $L_s = 54$ mm. The space ratio S is defined as $S = L_h/L_s$ [30].

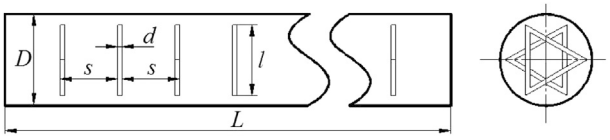

Fig. 8. Triangle circular poles in a tube.

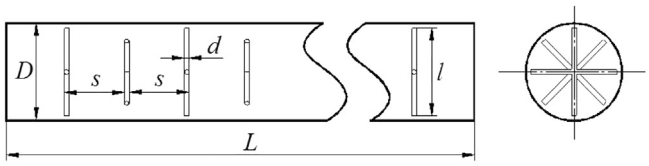

Fig. 9. Ten crossing circular poles in a tube.

As shown in Fig. 13, heat transfer performance of full-length screw-tapes is slightly better than that of regularly-spaced helical screw-tapes, corresponding to β. The reductions of Nusselt number for the regularly-spaced helical screw-tapes are 11%–15% based on various Reynolds numbers in comparison with the full-length helical screw-tapes. For full-length helical screw-tapes inserting a tube, Nusselt number reaches about 120 and synergy angle β reaches about 78° when $Re = 1800$. The reductions of friction factor of regularly-spaced helical screw-tapes are 43%–53% on various Reynolds numbers in comparison with the full-length helical screw-tapes, corresponding to θ. For regularly-spaced helical screw-tapes inserting a tube, the friction coefficient reaches about 0.52 and synergy angle θ reaches about 60° when $Re = 1800$.

Fig. 14 shows the relation of *EEC* value with Reynolds number for two models of helical screw-tapes in a tube. As shown in the figure, the *EEC* value of two models in a tube increases with Reynolds number ranging from 300 to 1200 and remains nearly constant after Reynolds number exceeds 1200. The model gives the maximum *EEC* value 0.91 when $Re = 1800$. Accordingly, inserting helical tapes in a tube is a promising technique for heat transfer enhancement.

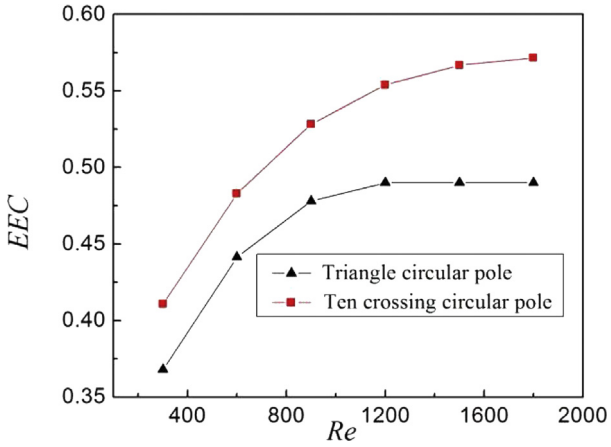

Fig. 11. Relation between *Re* and *EEC* value of heat transfer enhanced tube with triangle circular poles and ten crossing circular poles.

Fig. 15, i.e. comprehensive efficiency evaluation plot, reflects all working points of the models discussed above. Six working points for every additive are arranged ranging Reynolds number from 300 to 1800 from bottom up. For three regularly-spaced twisted tapes in tube, half of the working points are presented in region I, i.e. the *EEC* value of about half of the working points are larger than 1, with different distances between twisted tapes in the cross section. According to the intercept discussed before, *EEC* reaches the maximum value 1.194 when $a = 5$ mm and $Re = 1800$, which indicates that the ratio of heat transfer enhancement is 1.194 times as the ratio of power consumption increase for enhanced tube in

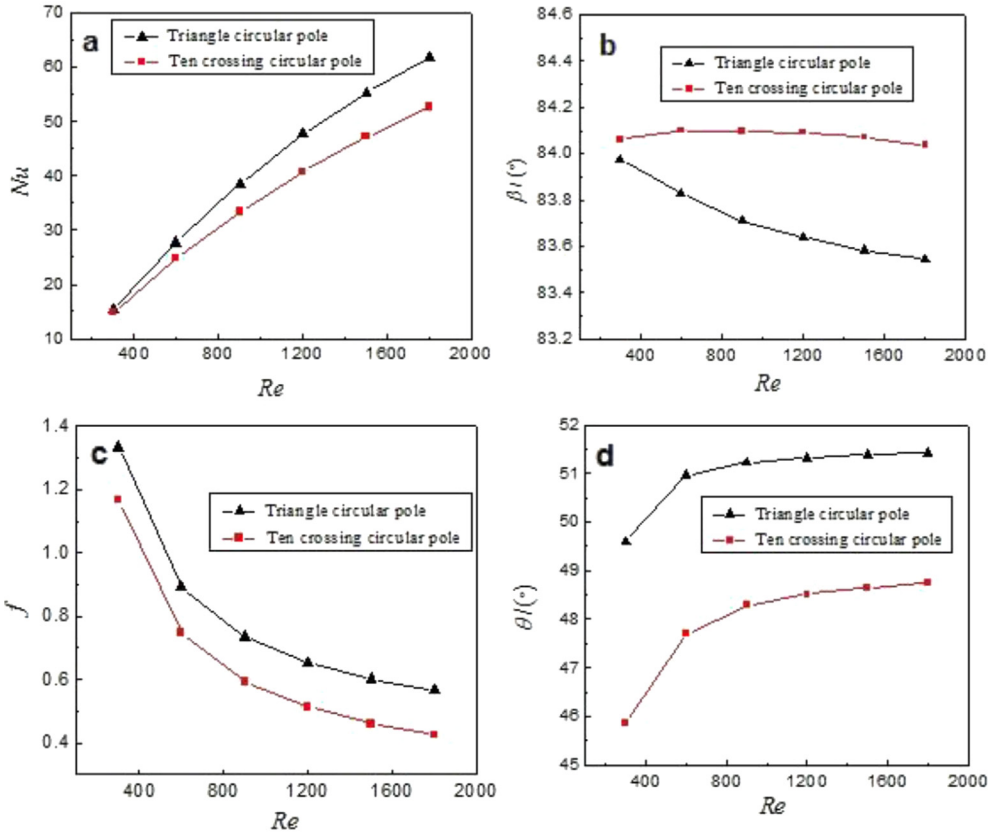

Fig. 10. Relation between *Re* and *Nu*, β, *f*, θ of heat transfer enhanced tube with triangle circular poles and ten crossing circular poles in (a), (b), (c), (d) respectively.

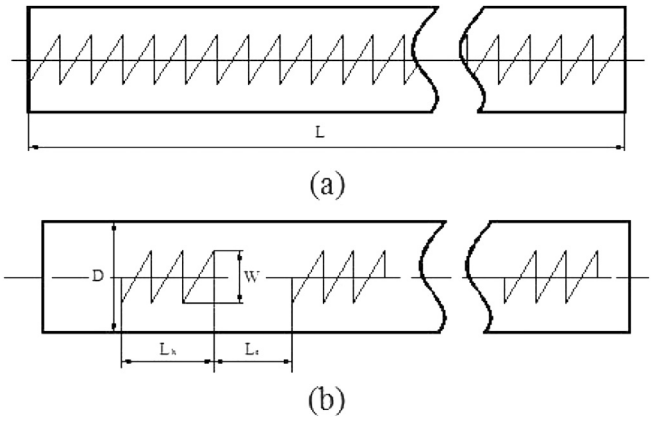

Fig. 12. Helical screw-tape in a tube, (a) Full-length helical screw-tape; (b) regularly-spaced helical screw tape.

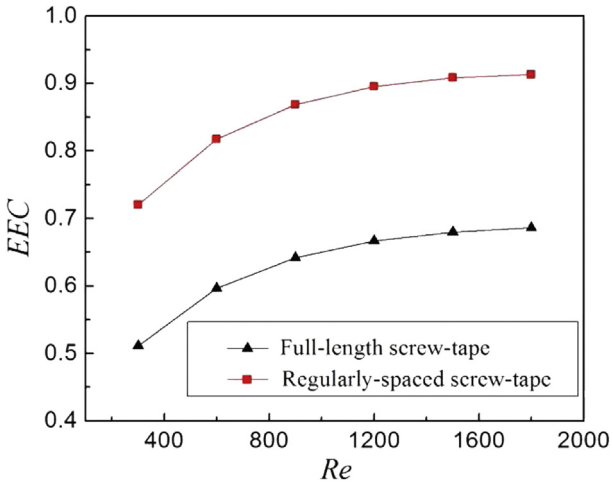

Fig. 14. Relation between *Re* and *EEC* value of heat transfer enhanced tube with helical screw-tapes.

comparison with a bare tube based on identical Reynolds number and identical dimensions. Therefore, inserting three regularly-spaced twisted tapes in a tube is a practical and applicable technique for heat transfer enhancement. Similarly, *EEC*, the ratio of heat transfer capacity increase over the ratio of power consumption increase for four regularly-spaced twisted tapes, triangle circular poles, ten crossing circular poles, full-length and regularly-spaced helical screw-tapes are presented in Fig. 15. As shown, working points of three regularly-spaced twisted tapes, four regularly-spaced twisted tapes and regularly-spaced helical tapes are plotted in or approaching region I, indicating they are effective ways to enhance heat transfer and save energy. Full-length helical screw-tapes have the similar value of Q/Q_0 but larger value of $\Delta P/\Delta P_0$ compared with regularly-spaced helical screw-tapes which results in lower comprehensive index *EEC*. This is because of the fact that the geometric arranging pattern of regular spaces reduces the pressure drop and thus increases comprehensive efficiency index, which corresponds with the core flow heat transfer enhancement proposed by Liu [4–6]. Every working point of triangle circular poles and cross circular poles is in region II and far away from baseline resulting from the two models lack of disturbance in fluid and increase flow resistance. The two models have smaller value of Q/Q_0 and larger value of $\Delta P/\Delta P_0$ in comparison with three regularly-spaced helical screw-tapes on identical Reynolds number, thus *EEC* of the two models is much smaller. Therefore, triangle circular poles and cross circular poles interpolating into a tube are not effective ways for heat transfer enhancement.

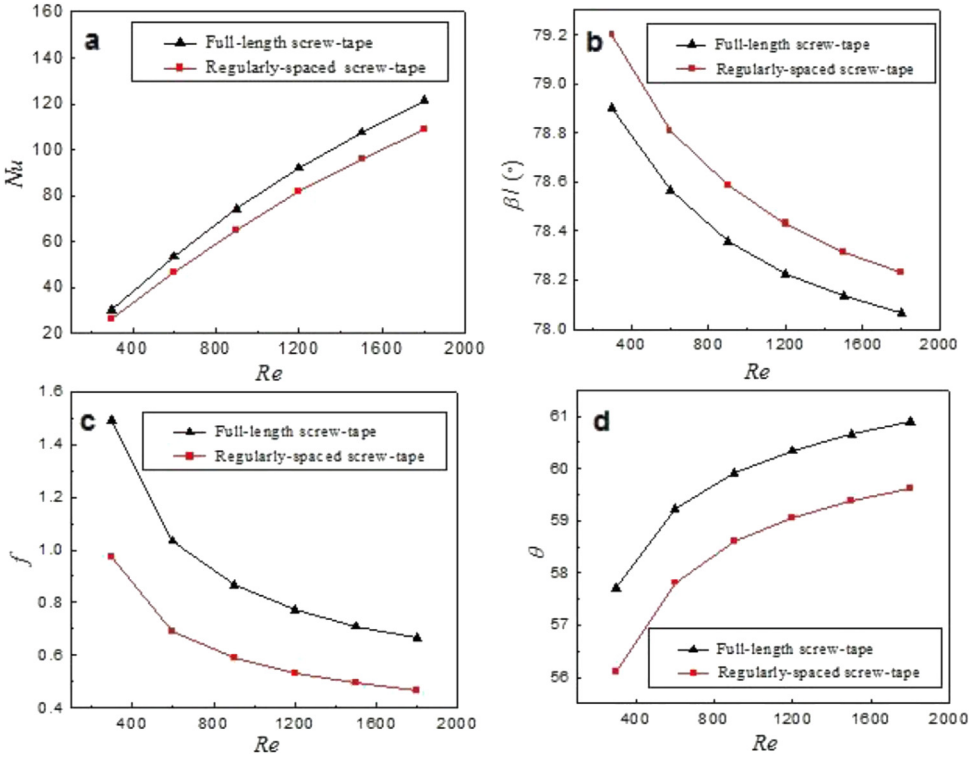

Fig. 13. Relation between *Re* and *Nu*, *β*, *f*, *θ* of heat transfer enhanced tube with helical screw tapes in (a), (b), (c), (d) respectively.

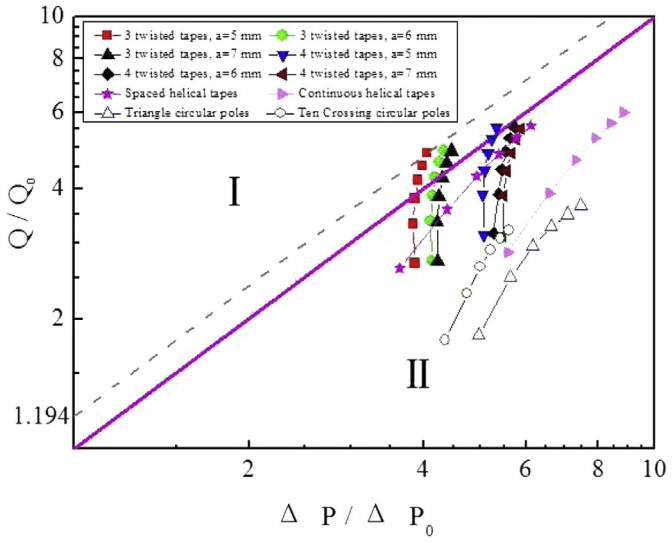

Fig. 15. An efficiency evaluation plot for enhancement techniques oriented for energy-saving.

6. Conclusions

Based on the analysis of internal relation of velocity and temperature field and velocity and pressure field for the convective heat transfer, the paper demonstrated multi-fields synergy principle and proposed relation between β and the heat transfer characteristics and relation between θ and the friction characteristics. The physical nature of heat transfer enhancement was presented through the analysis of synergy angle β and θ. By the comparison between the boundary flow heat transfer enhancement and the core flow heat transfer enhancement, inserting additives in the core flow region resulted in less friction and larger heat transfer rate. The comprehensive index *EEC* and efficiency evaluation plot were proposed. Various values of *EEC* and positions in comprehensive efficiency evaluation plot for various enhanced elements reflected the performance of different techniques. Numerical simulations of four typical additives in tube were provided to verify the relation between β and heat transfer performance and relation between θ and friction characteristics and all results were evaluated by the value of *EEC* and the efficiency evaluation plot.

Acknowledgments

This work was supported by the National Natural Science Foundation of China (No. 51036003) and the National Key Basic Research Development Program of China (No. 2013CB228302).

Nomenclature

a	distance between tapes in cross section [m]
A	heat transfer area [m^2]
c_p	specific heat [kJ/(kg K)]
D	tube diameter [m]
f	friction factor
k	thermal conductivity [W/m K]
L	flow channel length [m]
L_h	helical tape length [m]
L_s	free-spacing length [m]
Nu	Nusselt number
P	power consumption [W]
Pr	Prandtl number
Q	heat transfer rate [W]
Re	Reynolds number
s	tape to space ratio ($s = L_h/L_s$)
t	tape thickness [m]
T_w	wall temperature [K]
T_∞	inlet temperature of fluid [K]
T	temperature of fluid [K]
u	velocity along x direction [m/s]
u_m	average velocity of cross-section [m/s]
$\boldsymbol{U}$	flow velocity vector of fluid [m/s]
v	velocity along y direction [m/s]
V	volume flow rate
W	tape width [m]
∇P	pressure gradient [Pa/m]
Δp	pressure drop [Pa]
Δt	wall-to-fluid temperature difference [K]

Greek symbols

β	synergy angle [°]
θ	synergy angle [°]
ρ	fluid density [kg/m^3]
μ	dynamic viscosity [kg/(m s)]

Subscript

0	bare tube

References

[1] A.E. Bergles, ExHFT for fourth generation heat transfer technology, Exp. Therm. Fluid Sci. 26 (2002) 335–344.
[2] R.L. Webb, Principles of Enhanced Heat Transfer, Wiley, New York, 1994.
[3] A. Bejan, A.D. Kraus, Heat Transfer Handbook, John Wiley & Sons, New Jersey, 2003.
[4] W. Liu, K. Yang, Mechanism and numerical analysis of heat transfer enhancement in the core flow along a tube, Sci. China, Ser. E 51 (2008) 1195–1202.
[5] W. Liu, K. Yang, Z.C. Liu, Mechanism of heat transfer enhancement in the core flow of a tube and its numerical simulation, Open Transp. Phenom. J. 2 (2010) 9–15.
[6] W. Liu, Z.C. Liu, Y.S. Wang, Flow mechanism and heat transfer enhancement in longitudinal-flow tube bundle of shell-and-tube heat exchanger, Sci. China, Ser. E 52 (2009) 2952–2959.
[7] Z.Y. Guo, D.Y. Li, B.X. Wang, A novel concept for convective heat transfer enhancement, Int. J. Heat Mass Transfer 41 (1998) 2221–2225.
[8] Z.Y. Guo, W.Q. Tao, R.K. Shah, The field synergy (coordination) principle and its applications in enhancing single phase convective heat transfer, Int. J. Heat Mass Transfer 48 (2005) 1797–1807.
[9] W.Q. Tao, Y.L. He, A unified analysis on enhancing single phase convective heat transfer with field synergy principle, Int. J. Heat Mass Transfer 45 (2002) 4871–4879.
[10] L.D. Ma, Z.Y. Li, W.Q. Tao, Experimental verification of the field synergy principle, Int. Commun. Heat Mass Transfer 34 (2007) 269–276.
[11] W.Q. Tao, Z.Y. Guo, et al., Field synergy principle for enhancing convective heat transfer-its extension and numerical verifications, Int. J. Heat Mass Transfer 45 (2002) 3849–3856.
[12] J.M. Wu, W.Q. Tao, Investigation on laminar convection heat transfer in fin-and-tube heat exchanger in aligned arrangement with longitudinal vortex generator from the viewpoint of field synergy principle, Appl. Therm. Eng. 27 (2007) 2609–2617.
[13] L.T. Tian, Y.L. He, Numerical study of fluid flow and heat transfer in a flat-plate channel with longitudinal vortex generators by applying field synergy principle analysis, Int. Commun. Heat Mass Transfer 36 (2009) 111–120.
[14] Y.B. Tao, Y.L. He, Three-dimensional numerical study and field synergy principle analysis of wavy fin heat exchangers with elliptic tubes, Int. J. Heat Fluid Flow 28 (2007) 1531–1544.
[15] P. Chu, Y.L. He, Three-dimensional numerical study on fin-and-oval-tube heat exchanger with longitudinal vortex generators, Appl. Therm. Eng. 29 (2009) 859–876.
[16] W. Liu, Z.C. Liu, Physical quantity synergy in laminar flow field and its application in heat transfer enhancement, Int. J. Heat Mass Transfer 52 (2009) 4669–4672.
[17] W. Liu, Z.C. Liu, Z.Y. Guo, Physical quantity synergy in laminar flow field of convective heat transfer and analysis of heat transfer enhancement, Chin. Sci. Bull. 54 (2009) 3579–3586.
[18] W. Liu, Z.C. Liu, S.Y. Huang, Physical quantity synergy in the field of turbulent heat transfer and its analysis for heat transfer enhancement, Chin. Sci. Bull. 55 (2010) 2589–2597.

[19] A. Bejan, General criterion for rating heat exchanger performance, Int. J. Heat Mass Transfer 21 (1978) 655–658.
[20] R.O. William, A. Bejan, Conservation of available work (exergy) by using promoters of swirl flow in forced convection heat transfer, Energy 5 (1980) 587–596.
[21] A. Bejan, Second law analysis in heat transfer, Energy 5 (1980) 721–732.
[22] J.F. Fan, W.K. Ding, J.F. Zhang, Y.L. He, A performance evaluation plot of enhanced heat transfer techniques oriented for energy-saving, Int. J. Heat Mass Transfer 52 (2009) 33–44.
[23] R.L. Webb, E.R. Eckert, Applications of rough surfaces to heat exchanger design, Int. J. Heat Mass Transfer 15 (1972) 1647–1658.
[24] R.L. Webb, Performance evaluation criteria for use of enhanced heat transfer surfaces in heat exchanger design, Int. J. Heat Mass Transfer 24 (1981) 715–726.
[25] W. Liu, Z.C. Liu, L. Ma, Application of a multi-field synergy principle in the performance evaluation of convective heat transfer enhancement in a tube, Chin. Sci. Bull. 57 (2012) 1600–1607.
[26] W. Liu, S. Shen, S.B. Riffat, Heat transfer and phase change of liquid in an inclined enclosure packed with unsaturated porous media, Int. J. Heat Mass Transfer 45 (2002) 5209–5219.
[27] Z.F. Huang, A. Nakayama, K. Yang, C. Yang, W. Liu, Enhancing heat transfer in the core flow by using porous medium insert in a tube, Int. J. Heat Mass Transfer 53 (2010) 1164–1174.
[28] X.Y. Zhang, Z.C. Liu, W. Liu, Numerical studies on heat transfer and flow characteristics for laminar flow in a tube with multiple regular spaces twisted tapes, Int. J. Therm. Sci. 58 (2012) 157–167.
[29] X.Y. Zhang, Z.C. Liu, W. Liu, Numerical studies on heat transfer and friction factor characteristics of a tube fitted with helical screw-tape without core-rod inserts, Int. J. Heat Mass Transfer 60 (2013) 490–498.
[30] S. Eiamsa-ard, P. Promvonge, Enhancement of heat transfer in a tube with regularly-spaced helical tape swirl generators, Sol. Energy 78 (2005) 483–494.